

Journal Pre-proof

Optimization of mixture proportions by statistical experimental design using response surface method - A review

Zhiping Li, Dagang Lu, Xiaojian Gao



PII: S2352-7102(20)33733-5

DOI: <https://doi.org/10.1016/j.jobe.2020.102101>

Reference: JOBE 102101

To appear in: *Journal of Building Engineering*

Received Date: 24 September 2020

Revised Date: 17 November 2020

Accepted Date: 14 December 2020

Please cite this article as: Z. Li, D. Lu, X. Gao, Optimization of mixture proportions by statistical experimental design using response surface method - A review, *Journal of Building Engineering*, <https://doi.org/10.1016/j.jobe.2020.102101>.

This is a PDF file of an article that has undergone enhancements after acceptance, such as the addition of a cover page and metadata, and formatting for readability, but it is not yet the definitive version of record. This version will undergo additional copyediting, typesetting and review before it is published in its final form, but we are providing this version to give early visibility of the article. Please note that, during the production process, errors may be discovered which could affect the content, and all legal disclaimers that apply to the journal pertain.

© 2020 Published by Elsevier Ltd.

1 1

2 **Optimization of mixture proportions by statistical experimental design using** 3 **response surface method - A review**

4 Zhiping Li¹, Dagang Lu^{1,2,3,*}, Xiaojian Gao^{1,2,*}

5 1. *School of Civil Engineering, Harbin Institute of Technology, Harbin 150090, China*

6 2. *Key Lab of Structures Dynamic Behavior and Control of the Ministry of Education, Harbin Institute of*
7 *Technology, Harbin 150090, China*

8 3. *Key Lab of Smart Prevention and Mitigation of Civil Engineering Disasters of the Ministry of Industry*
9 *and Information Technology, Harbin Institute of Technology, Harbin 150090, China*

10

11 **Abstract:** A comprehensive review of the statistical experimental optimization
12 problem concerning the mixture design of various cement-based materials is
13 presented herein. This review summarizes and discusses over 80 applications of
14 optimum design regarding the basic test information under response surface method
15 (RSM), including influence factor and corresponding response, statistical method,
16 and coefficient of determination. The statistical experimental design reported in
17 previous studies has shown that RSM is a sequential procedure to provide a suitable
18 approximation for the mixture optimization. Then, linear, quadratic and interactive
19 relationships of the statistical model can be evaluated available. Especially, the
20 multi-objective optimization issues with multiple or competing performance
21 requirements for various cement-based materials have also been reported, by
22 considering fluidity, strength development, environmental impact, cost and durability.
23 Overall, the results from existing publications have demonstrated that statistical
24 inference and analysis of variance (ANOVA) are suitable for mix proportion design

* Corresponding author.

E-mail address: ludagang@hit.edu.cn (D. Lu); gaoxj@hit.edu.cn (X. Gao)

25 and process optimization of cement-based materials. The W/B ratio and mixture
26 components are the prevalent factors in experimental design optimization, and then the
27 fluidity and strength as the most popularly used response. Thus, theoretical optimum
28 mixture proportioning can be used to predict valuable fresh and hardened properties.
29 Finally, a critical discussion of the selection of design strategy, independent factors
30 and their responses, and the experimental region involved in statistical experimental
31 design, is provided. Based on this review, we conclude that the multi-objective
32 optimization approaches need a further systematic study, and further studies of
33 sustainable concrete optimization are needed by comparing the different chemical
34 composition and particle characteristics.

35 **Keywords:** *experimental design optimization; supplementary cementitious materials*
36 *(SCMs); response surface methodology (RSM); sustainable concrete; ultra-high*
37 *performance concrete (UHPC)*

38 1. Introduction

39 The cement-based materials are prepared by using various types and quantities of
40 individual constituents. These mixture proportions play an important role in fresh- and
41 hardened-state performance, such as fluidity, rheological properties, strength development and
42 durability. Therefore, many research studies have been dedicated to experimental optimization
43 of cement and concrete mixtures.

44 Experimental design optimization is an adjustment process of selecting the available
45 proportion of raw materials to prepare a cement-based mixture that satisfies specifiable
46 requirements for a particular application. Generally, conventional optimization for mixture
47 design can be classified as prescriptive and performance-based approaches [1].
48 Prescriptive-based methods are often stepwise selection to provide a mixture for a particular
49 application, thereby satisfying the current mix proportion design standards and specifications,
50 such as JGJ 55 [2] for concrete, JGJ/T 98 [3] for mortar, and JGJ/T 233 [4] for cement. The
51 main advantage of these methods is that the mixture proportion is provided by the national or
52 industry standard solely, not entirely depending on personal experience and subjective
53 decision. Performance-based techniques emphasize no strict requirements on the type and
54 quantities of components, but are designed with many laboratory trial experiments (defined as
55 trial-and-error method). Trial-and-error or single variable method suffers from an exponential
56 growth in experimental times when many test factors are considered as independent variables
57 in the optimization process. Furthermore, detailed optimization designs of concrete mixtures
58 are often time- and resource-intensive [1]. Response surface method (RSM) is a combination
59 of mathematical and statistical techniques that are widely used in the area of concrete
60 preparation optimization, where some nonlinear factors of concrete are added to obtain an
61 optimum domain [5]. This method is especially suitable for multiple performance

62 requirements of concrete, such as ultra-high performance concrete (UHPC) [6-9]. Over the
63 past decade, the statistical experimental design of cement-based materials has gained
64 increasing attention with the sustainable development of the concrete industry. Among these,
65 lots of researchers have investigated the optimization of mixture proportions by using RSM.

66 Recently, the multiple response problem of cement-based materials has been widely
67 reported in previous experimental studies. The simultaneous optimization process of several
68 responses can be classified into two steps, as follows: (1) a fitting response surface model is
69 established for every response, and (2) operating constraints optimized by all responses are
70 identified or maintained in the desired region. Some related optimization methods, such as
71 D-optimal design [10], overlay of the contour plots and constrained optimization, have been
72 used in previous studies. Overlaying contour plots work effectively for a small number of
73 design variables. If more than three independent factors exist, then this method is ineffective
74 because the two-dimensional contour plot cannot obtain the best view of the response surface.
75 The two other approaches can be used for cases with more variables.

76 This paper summarizes and discusses the main achievements including the applications of
77 different RSMs and optimization methodologies in the experimental design of cement-based
78 materials. This review is organized as follows. The basic procedure and certain theoretical
79 models and its evaluation and validation are reviewed briefly in Section 2. Then, in Section 3,
80 the typical applications of central composite design (CCD) and other optimization designs are
81 summarized and investigated to measure the feasibility and validity of the selected RSM,
82 especially for the sustainable concrete application. Finally, in Section 4, several related
83 problems for further promising applications of RSMs in cement-based materials are
84 discussed.

85 **2. Theoretical basis of RSM for cement-based materials**

86 2.1 General procedure using RSM in experimental design optimization

87 RSM has been used for various issues in the experimental optimization of cement-based
 88 materials [11]. This method aims to optimize mixture design to consider several attributes,
 89 involving workability, strength development, cost, durability and environmental impact. These
 90 features are achieved with sequential experimentation including factors such as water–binder
 91 ratio (W/B), mixture constituent, the proportion of supplementary cementitious materials
 92 (SCMs), preparation conditions and curing environment. In general, if the response is well
 93 expressed by a linear model of the independent factors, then the first-order regression model
 94 can be expressed as follows:

$$95 \quad Y = \beta_0 + \sum_{i=1}^k \beta_i X_i + \varepsilon, \quad (1)$$

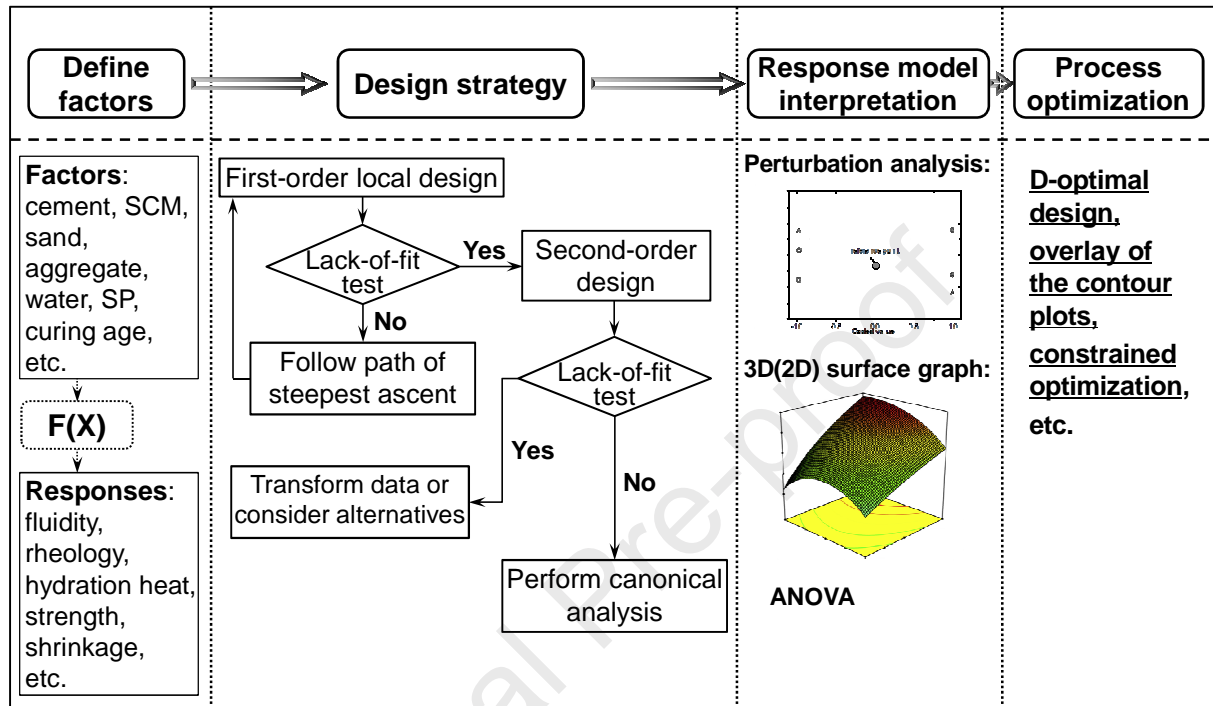
96 where Y represents the response variable conforming to the regression coefficients (β); X_i
 97 represent the independent variables; k is the number of optimized variables; ε denotes the
 98 random error of the estimated response. If a curvature is found in the local experiments, then a
 99 second-order regression model can be given as follows:

$$100 \quad Y = \beta_0 + \sum_{i=1}^k \beta_i X_i + \sum_{i=1}^k \beta_{ii} X_i^2 + \sum_{i=1}^k \sum_{j>1}^k \beta_{ij} X_i X_j + \varepsilon, \quad (2)$$

101 where the regression coefficients are expressed as β_0 for the intercept term, β_i for the
 102 first-order terms, β_{ii} for the quadratic terms and β_{ij} for the binary-interaction terms. A
 103 polynomial function cannot be a suitable approximation for all independent variable spaces.
 104 However, they usually work comparatively well for a relatively small area [12].

105 The main purpose of experimental optimization is to move quickly to the actual optimum
 106 by using a simple and economically experimental process [13]. The general flow chart of RSM
 107 for experimental design optimization can be summarized in Fig. 1. The design procedure by
 108 using RSM consists of the following sequential steps: (1) defining independent factors and

109 desired responses, (2) selecting appropriate design strategy to fit the response surfaces, (3)
 110 confirming the fitted model by using analysis of variance (ANOVA) and statistical inference,
 111 and (4) determining the optimum set of operating conditions.



112

113 **Fig. 1** General flow chart of RSM in experimental design optimization.

114 2.2 Designs of the first-order model

115 Designs for fitting the first-order model are called first-order designs. The most widely
 116 used first-order designs are 2^k factorial design, Plackett–Burman design and simplex design
 117 [14]. Among these designs, simplex lattice design has obtained considerable attention in the
 118 experimental design optimization of cement-based materials, which are described briefly in the
 119 following section.

120 Simplex lattice design is used to investigate the effects of the components or ingredients of
 121 a mixture on the response variable; it is also referred to as the mixture experiment. In general,
 122 the key feature of the given mixtures is that the volume or mass fractions of these components
 123 must sum to one. Furthermore, the response of the given mixture depends only on the relative

124 fraction but not on the total amount of the mixture constituents [15]. For instance, if x_1, x_2, \dots, x_k
 125 represent the proportions of k ingredients of the given mixture, then

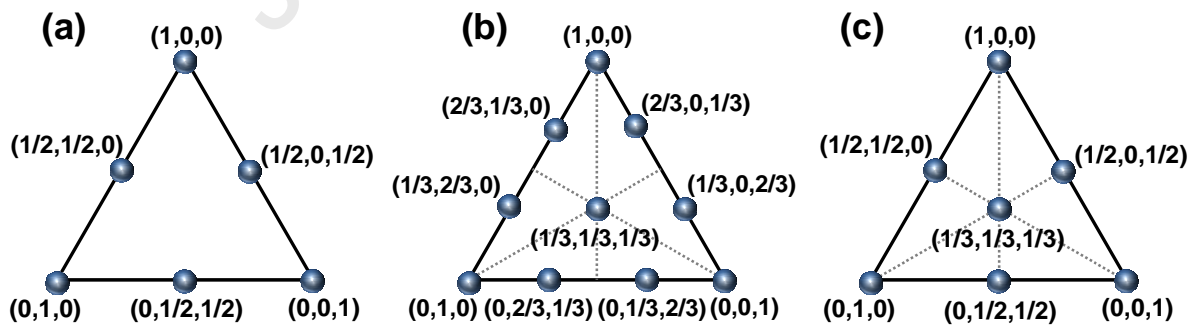
$$126 \quad 0 \leq x_i \leq 1 \quad (i = 1, 2, \dots, k), \quad (3)$$

$$127 \quad \text{and} \quad \sum_{i=1}^k x_i = 1. \quad (4)$$

128 Moreover, some additional boundary constraints are found on the components, thereby
 129 limiting the available region of the ingredients between the lower limit (L_i) and the upper limit
 130 (T_i). The general form of the mixture optimization could be expressed as follows:

$$131 \quad 0 \leq L_i \leq x_i \leq T_i \leq 1 \quad (i = 1, 2, \dots, k). \quad (5)$$

132 The main types of simplex lattice designs in previous articles are shown in Fig. 2. The
 133 points presented in Fig. 2 denote experimental runs, and the three vertices, midpoints of the
 134 sides and the overall centroid of the triangle represent the pure blends, binary blends and
 135 ternary blends, respectively. The controversy of the simplex lattice design is that most test runs
 136 emerge in the boundary of the optimized area. Simplex lattice and simplex centroid design
 137 should be added with points in the internal region, as shown in [16].

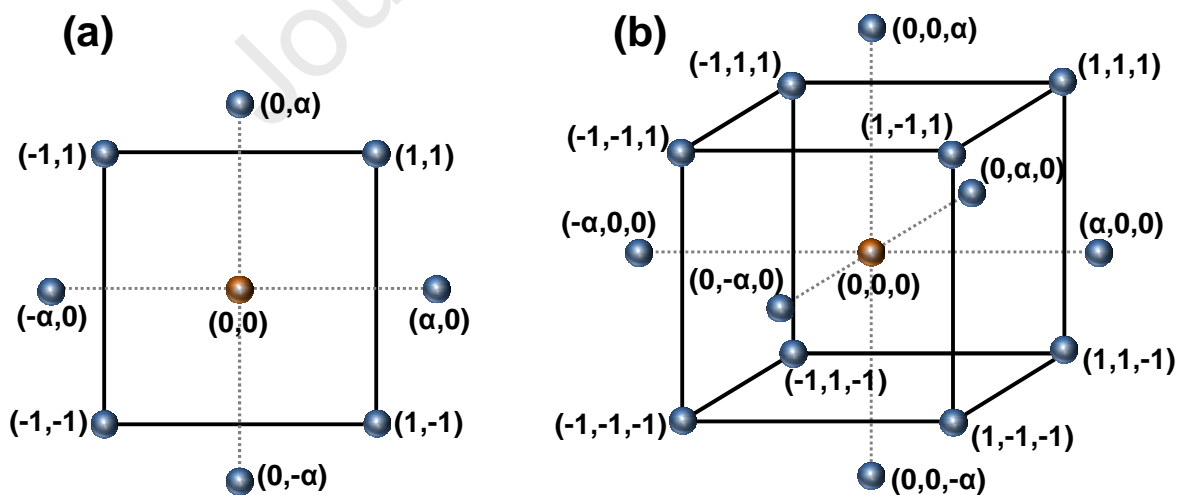


138
 139 **Fig. 2** Simplex lattice designs for three-component mixture plans: (a) [3,2] lattice, (b) [3,3]
 140 lattice, and (c) simplex centroid.

141 2.3 Designs of the second-order model

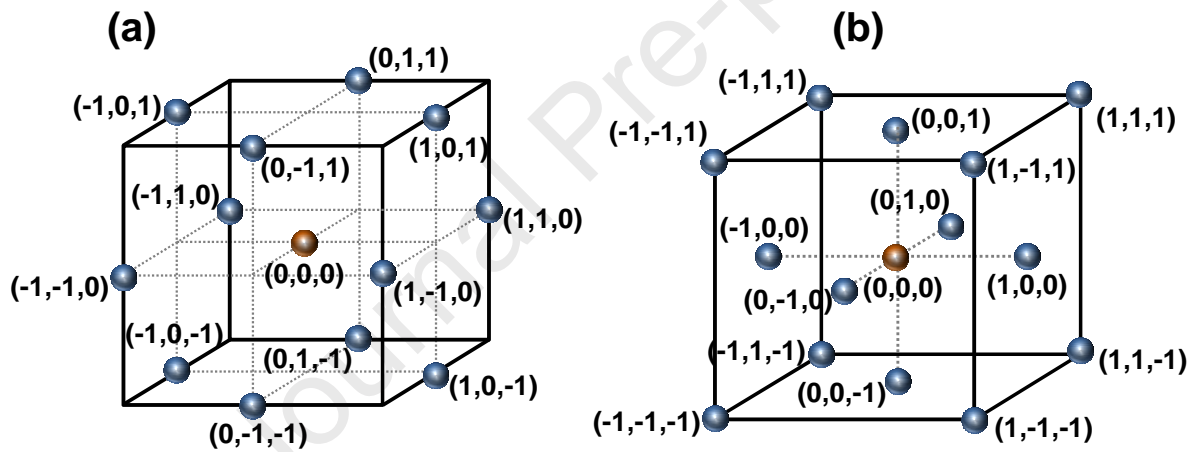
142 Designs for fitting the second-order model are called second-order designs. Applications
 143 of CCD and Box–Behnken design (BBD) to cement and concrete have become more
 144 increasingly popular over the past few decades.

145 CCD include 2^k factorial runs, $2k$ star runs and k_0 runs (centre-point replications, usually
 146 $3 \leq k_0 \leq 5$); it is a good alternative to the 3^k full factorial design because it provides
 147 comparable experimental results with a small number of tests [17]. Fig. 3 shows a CCD for the
 148 case of $k=2$ and $k=3$. In general, CCD is developed in a manner of the sequential
 149 experiment to investigate a first-order design, followed by adding axial runs to fit the
 150 second-order model. The first-degree model is used to obtain initial information on the
 151 experimental programs and to assess the importance of the component of the given mixture.
 152 Then, the quadratic terms are chosen to obtain additional information to determine the desired
 153 properties of the given constraints. The value of α and k_0 depend on the number of runs in the
 154 factorial region of the given experiment to ensure that CCD can achieve either the orthogonality
 155 behaviour or uniform precision behaviour.



156
 157 **Fig. 3** Central composite designs for (a) $k=2$ variables and (b) $k=3$ variables of
 158 experimental optimization (The red dot is the centre-point replication, generally, $3 \leq k_0 \leq 5$).

159 BBD consists of 2^k factorial three-level designs with incomplete block to afford as either
 160 rotatable or nearly rotatable properties and to avoid the vertices of the cubic region, as shown
 161 geometrically in Fig. 4a. All points of BBD located at a spherical region of radius $\sqrt{2}$, to avoid
 162 the upper and lower limits of the given constraints. In addition, this would be available for BBD
 163 when the extreme vertices are prohibitively expensive or impossible to complete owing to the
 164 constraints of the experimental conditions. Face-centred design (CCF) is a useful variation of
 165 CCD, where $\alpha = 1$. Fig. 4b shows the star points of CCF located at the centre of the surface of
 166 the cube region, instead of the spherical area as in CCD. Using CCF often leads to a reasonable
 167 assessment of experimental errors because of more centre runs.



168
 169 **Fig. 4** Spherical designs for three variables: (a) Box-Behnken design, and (b) face-centred
 170 central composite design (The red dot is the centre-point replication, generally, $3 \leq k_0 \leq 5$).

171 2.4 Evaluation and validation of the fitting model

172 ANOVA is most often used to validate the predictive ability of the fitted model before
 173 prediction, to ensure that the mathematical model provides an adequate approximation of the
 174 actual response behaviour. The ANOVA expressions for regression model assessment and
 175 validation are summarised in Table 1. In general, the overall accuracy of the predicted model is
 176 often described by the coefficient of determination R^2 , which is calculated as follows:

$$R^2 = \frac{SS_{\text{mod}}}{SS_{\text{tot}}} = 1 - \frac{SS_{\text{res}}}{SS_{\text{tot}}}. \quad (6)$$

The value of R^2 varies between 0 and 1. For the predicted model with good accuracy, the value of R^2 is close to 1. After considering the number of model terms, a related statistic parameter of adjusted R^2 can be obtained, as follows:

$$R_{\text{adj}}^2 = 1 - \frac{MS_{\text{res}}}{MS_{\text{tot}}} = 1 - \frac{SS_{\text{res}}/(k-p)}{SS_{\text{tot}}/(k-1)}. \quad (7)$$

The value of R_{adj}^2 decreases as statistically insignificant variables in the model increase. The differences between the predicted and the actual values are defined as residual errors, which play a critical role in evaluating the model accuracy. Another statistic used to measure the predictive ability of the model, is expressed as follows:

$$R_{\text{pre}}^2 = 1 - \frac{SS_{\text{pre}}}{SS_{\text{tot}}}. \quad (8)$$

The value of R_{pre}^2 and R_{adj}^2 should be within 0.2.

Table 1 Basic structure of the ANOVA test in the RSM-based experimental design.

Source of variation	Degrees of freedom	Sum of squares	Mean square	F-value
Total corrected	$k-1$	$SS_{\text{tot}} = \sum_{i=1}^k (y_i - \bar{y})^2$		
Model	$p-1$	$SS_{\text{mod}} = SS_{\text{tot}} - SS_{\text{res}}$	$MS_{\text{mod}} = SS_{\text{mod}}/(p-1)$	$MS_{\text{mod}}/MS_{\text{res}}$
Residual	$k-p$	$SS_{\text{res}} = \sum_{i=1}^k (y_i - \hat{y}_i)^2$	$MS_{\text{res}} = SS_{\text{res}}/(k-p)$	
Lack of fit	$m-p$	$SS_{\text{lof}} = SS_{\text{res}} - SS_{\text{pe}}$	$MS_{\text{lof}} = SS_{\text{lof}}/(m-p)$	$MS_{\text{lof}}/MS_{\text{pe}}$
Pure error	$k-m$	$SS_{\text{pe}} = \sum_{i=1}^m \sum_{j=1}^{k_i} (y_{ij} - \bar{y}_i)^2$	$MS_{\text{pe}} = SS_{\text{pe}}/(k-m)$	

Note: k = total number of experiments in the set; p = total number of parameters in the model; m = number of distinct level of factor combinations; k_i = number of replications of the i th level; Adapted from [18]

Desirability function is another useful method to optimize multiple responses simultaneously. Thus, this approach tends to satisfy each desirable response as soon as possible

194 without excessively compromising any performance specifications. In general, every response
 195 Y_i is transformed into an individual desirability function as:

$$196 \quad 0 \leq d_i(Y_i) \leq 1, \quad (9)$$

197 where the value of $d_i(Y_i)$ ranges between 0 and 1. For the combination of the single responses
 198 near to the target values, the value of $d_i(Y_i)$ should be close to 1. The composite desirability
 199 function D can be expressed as follows:

$$200 \quad D = (d_1(Y_1), d_2(Y_2), \dots, d_k(Y_k))^{1/k} = \prod_{i=1}^k d_i(Y_i)^{1/k}, \quad (10)$$

201 where k represents the total responses involved in the optimization process.

202 **3. Literature survey of RSM in mixture design optimization**

203 In a review article published in 1999 [11], RSM is the first time systematically discussed
 204 and compared in mixture design optimization of high-performance concrete, and the
 205 multi-objective optimization by using material science-based statistical models is also
 206 presented to predict the concrete properties. Then, a comprehensive review of linear
 207 combination, statistical models, artificial intelligence method, and physics-based models was
 208 provided to optimize the design and proportioning of the concrete mixture [1]. Based on the
 209 previously surveyed, this paper attempted to evaluate the advances in cement and concrete
 210 mixture optimization by using RSM over the past two decades. Symbols used in this review
 211 are listed in Appendix A. Applications of RSM of mixture optimization of cement-based
 212 materials are shown in Appendix B.

213 Since the experimental results of Appendix B were obtained by various characteristics of
 214 raw materials and under various preparing conditions, this paper only collected the basic test
 215 information (influence factor and corresponding response, statistical method and coefficient

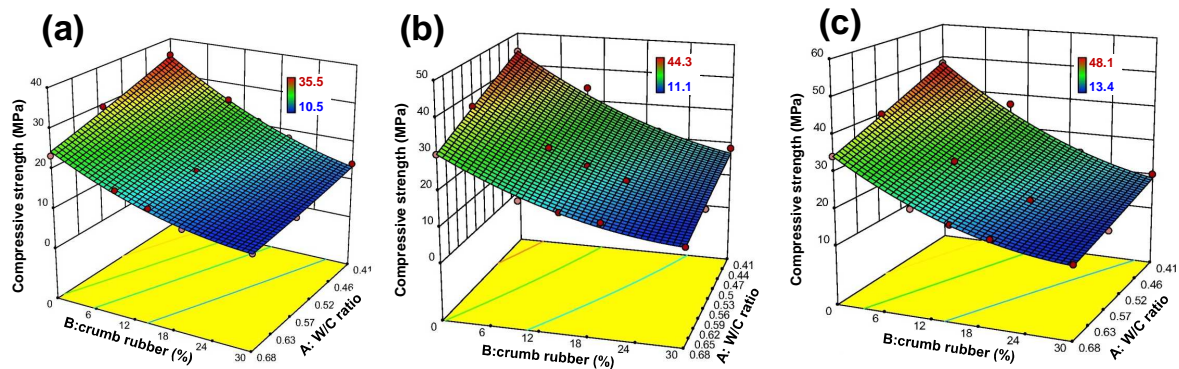
216 of determination) for further discussion. For more corresponding details of the tests, one can
217 refer to the references.

218 **3.1. Optimization designs in cement-based materials applications**

219 Over the past two decades, many studies on cement-based materials have focused on
220 using RSM as a secondary analysis in multi-objective optimization that can be achieved with
221 a series of separate experiments. This tool has been used successfully by previous researchers
222 to optimize fresh and hardened properties for cement and concrete fields. However, mixture
223 designs of some advanced cement-based materials are always difficult to standardize and
224 reproduce owing to lack of available guidelines [19]. Herein, the focus is on summarizing the
225 RSM applications; and the existing methods, including CCD, BBD and CCF are discussed in
226 the following sub-sections.

227 *3.1.1 Central composite design (CCD)*

228 CCD is the most commonly used method of experimental optimization in the
229 cement-based material field, which is used for fitting the second-order model. CCD is often
230 used as a screening design to determine the critical factors and their interactions. As an
231 example, Mohammend et al. [20] used CCD in modelling the fresh and hardened performance
232 of rubbercrete mixture to develop available mix proportion. Two factors (W/B and crumb
233 rubber) with five levels were selected and 45 runs were performed in this research. The
234 response surface with three slump levels for compressive strength is presented in Fig. 5.



235

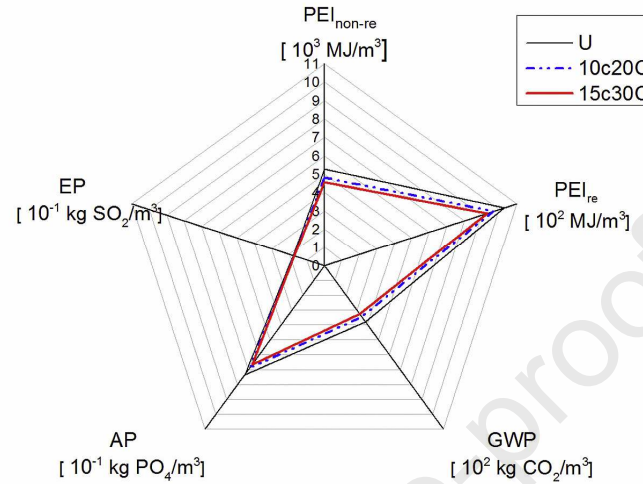
236 **Fig. 5** Response surface with three slump levels for compressive strength: (a) low slump, (b)
 237 medium slump and (c) high slump. Adapted from [20].

238 Based on the previous CCD applications shown in Appendix B. the existing studies can
 239 be classified into three groups of research characteristics, as follows: (1) optimizing the raw
 240 materials and preparation condition to achieve the optimal performance or the most
 241 economical mix design results, (2) adding new components to investigate the performance
 242 range, and (3) combining with other modelling techniques and then evaluating the feasibility.
 243 Especially, geopolymer/alkali-activated materials have acquired wide attention as promising
 244 construction and maintenance materials due to their superior performance [21]. Venkatesan et
 245 al. [22] applied CCD to determine the optimal conditions of geopolymer concrete by using
 246 partial replacement of fine aggregate with waste foundry sand and fly ash (FA). Then,
 247 D-optimal design was used to conduct the proportion of mixture components to acquire the
 248 desired responses. Mohammed et al. [23] optimized the experimental parameters of
 249 ingredients, such as anhydrous sodium metasilicate, ground granulated blast-furnace slag
 250 (GGBS) and FA to produce cast in situ alkali-activated binders. The optimal condition was
 251 provided using CCF to evaluate the three responses (split tensile strength, compressive
 252 strength and water absorption). Da Silva Alves et al. [24] investigated the effect of sisal fibre,
 253 activator–metakaolin mass ratio, and curing time on toughness and modulus of elasticity. In
 254 addition, the optimization of the experimental parameters was conducted by CCD combined

255 with canonical analysis to maximize the toughness and modulus of elasticity of the fibre
256 metakaolin-based geopolymer. Zahid et al. [25] applied CCD technique to establish the effect
257 of independent factors (NaOH molarity, NaOH–Na₂SiO₃ ratio and curing temperature) to
258 evaluate several responses (such as setting time, modulus of elasticity, compressive strength,
259 flexural strength, flexural toughness and ductility index) of FA-based engineered geopolymer
260 composite. CCD was used to confirm the optimal mixture parameter of alkali-activated slag
261 mortar with the maximum flexural strength and compressive strength, by considering the
262 influence of usage of waste glass powder [26]. Revathi et al. [27] used CCD to establish the
263 regression model of three factors (modulus of sodium silicate, liquid–FA ratio and mineral
264 admixture) and these interactions with mechanical strength with 15 experimental trials.

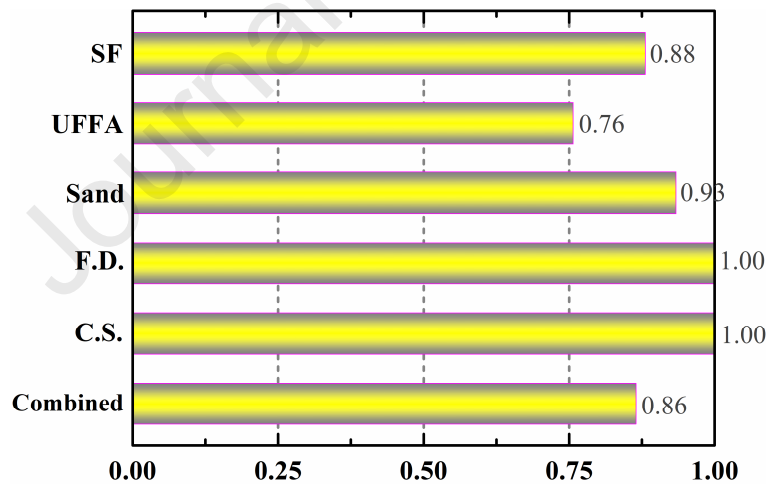
265 UHPC is characterized by dense microstructures that possess ultra-high mechanical,
266 ductility and durability performance. The optimization approach often starts with a
267 combination of particle packing and statistical design method to obtain a mixture proportion
268 of UHPC. The effects of three factors (distribution modulus, SCM and W/B ratio) on the
269 rheological and mechanical properties of strain-hardening UHPC were optimized by
270 combining CCD and modified Andreasen and Andersen particle packing model [28]. Sun et al.
271 [29] used CCD to evaluate the effect of porous aggregate and shrinkage-reducing admixture
272 on autogenous shrinkage of UHPC by using the modified dense particle-packing model. Wang
273 et al. [30] used the modified Andreasen and Andersen particle packing models to achieve a
274 compacting binder matrix of eco-friendly UHPC. Then, CCF was applied by maximum use of
275 combined micro-coral sand and coral sand. The developed eco-friendly UHPC was evaluated
276 by using the environmental impact indicator with the radar map (Fig. 6). On the other hand,
277 the optimum design of UHPC usually diminishes the energy consumption and emissions of
278 CO₂ with the reduction of cement content. Ferdosian and Camoes [31] used CCD to
279 investigate the effect of SF, ultra-fine FA and sand of UHPC on fluidity and compressive

280 strength. Then, a multi-objective optimization was conducted, and the cost and environmental
 281 influences were optimized by the overall desirability (Fig. 7). Furthermore, CCD shows an
 282 excellent fitting effect on other experiments [32-36].



283

284 **Fig. 6** Ecological evaluation of eco-friendly ultra-high performance concrete with
 285 environmental impact indicator. Adapted from [30]



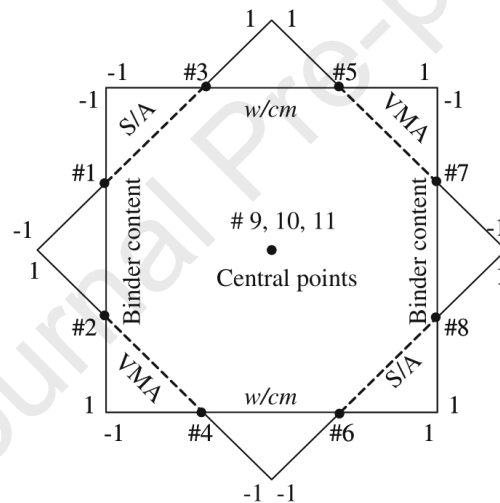
286

287 **Fig. 7** Desirability of ultra-high performance concrete for its main variable constituents.
 288 Adapted from [31]

289 3.1.2 Other optimization designs

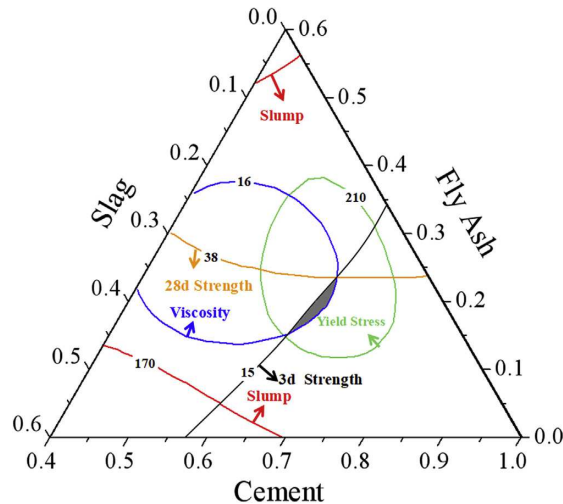
290 Factorial design is another method to optimize the mixture proportion of cement-based
 291 materials. It is often classified into two categories: full factorial design and fractional factorial
 292 design. Long et al. [37] applied fractional factorial design to build statistical models to

293 investigate the influence of mixture proportion and raw material properties on workability,
 294 strength development, and visco-elastic performance of self-compacting concrete. Then
 295 eleven additional SCC mixtures were used to validate the statistical models for fresh
 296 properties. Including eight runs within the range of the factorial design to develop the wide
 297 range, three central points were used to evaluate the error in the 90% confidence limit (Fig. 8).
 298 Jiao et al. [38] applied simplex centroid design to optimize the paste consisting of cement, FA
 299 and slag for a given strength grade, then optimized the paste, fine aggregate and coarse
 300 aggregate based on rheological properties of SCC, and at last, overlapped the contour plots to
 301 acquire the multiple performance requirements (Fig. 9).



302

303 **Fig. 8** Additional SCC mixtures used to validate the derived statistical models. Adapted from
 304 [37]



305

306 **Fig. 9** Optimization of cementitious materials composition by overlapping the contour plots.

307 Adapted from [38]

308 As for mix optimization of geopolymer/alkali-activated materials, Li et al. [39] proposed

309 a mixture proportioning methodology according to the performance requirements of

310 alkali-activated concrete and used the simplex centroid design for optimizing three types of

311 aggregates to obtain the optimized bulk density. Mermerdas et al. [40] applied simplex lattice

312 design to optimize three independent variables (curing age, curing temperature, and volume of

313 binder) of geopolymer mortars and to maximize the compressive strength of FA and GGBS.

314 Shi et al. [16] used simplex lattice design to correlate the ingredients of ternary cement blends

315 (cement, slag and FA) on ASR expansion with only seven experimental trials. Then, the

316 ternary contour diagram was used to analyse the composition effect on ternary composite

317 blends (Fig. 10). Li et al. [41] used BBD to investigate the effect of the degree of sol ratio, the

318 content of slag and age on fracture toughness and their interaction on fracture properties

319 before and after freeze-thaw resistance of alkali–slag concrete. Bektas et al. [42] used BBD to

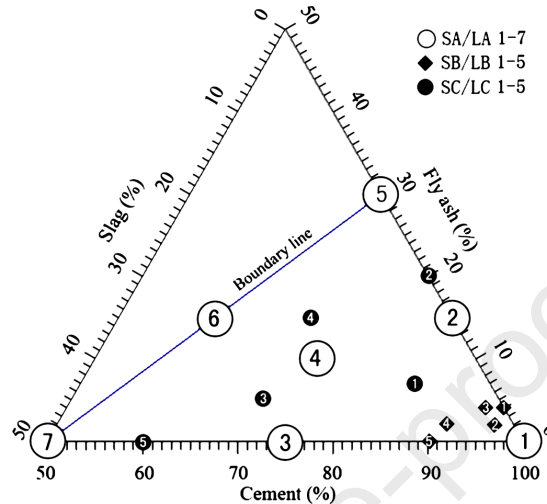
320 investigate the influence of three critical mix factors (alkali content, W/B ratio and ground

321 clay brick content) in three-levels to measure four responses (alkali–slag reaction expansion,

322 F_c , F_t and modulus of elasticity) in two replicates of 15 runs. Cai et al. [43] applied BBD to

323 analyse the influence of activator solution–slag ratio, sand ratio and slag content and their

324 interaction on the freeze-thaw cycles of the alkali-slag concrete. Then, the predicted model
 325 was built to evaluate the effect of air bubble characteristic on freeze-thaw cycles in cold
 326 regions.



327

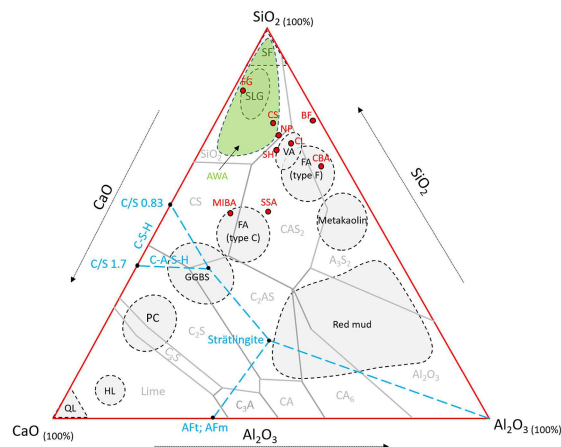
328 **Fig. 10** Ternary contour diagram of composition design for composite cement. Adapted from
 329 [16]

330 As for mix optimization of UHPC, Ghafari et al. [15] present an accurate analytical
 331 approach based on simplex lattice design to optimize the component of UHPC. The main
 332 strategy of this method can be described in seven steps, as follows: (1) constructing the main
 333 optimum objective to obtain the highest compressive strength, acceptable scope of
 334 workability and economical cost of raw materials; (2) selecting the mixture design method,
 335 where D-optimal techniques are recommended; (3) defining the constraint bounds of mixture
 336 components, parameters and these variation ranges in the defined experiments; (4) developing
 337 the design matrix based on the D-optimal mixture trials; (5) collecting the experimental data;
 338 (6) building the analytical model to predict the properties of UHPC; (7) optimizing the
 339 mixture proportion of UHPC to satisfy the desirable value of the response variable. Soliman
 340 and Tagnit-Hamou [44] proposed a modified approach combining a full-factorial design
 341 approach and particle-packing model to optimize UHPC as follows: (1) particle packing of

342 aggregates, and (2) building the optimized model by investigating the combined effect of W/B
 343 ratio and high range water-reducing admixture.

344 3.2. Optimization designs for sustainable concrete applications

345 Some industrial wastes are blended with cement clinker to prepare Portland cement or
 346 used as concrete constituents for sustainable application, which are widely investigated by
 347 academics and engineers. Existing experimental design of industrial wastes applications has
 348 attempted to explore the alternative of SCM and their performances in the concrete industry
 349 [22,26,30,31,33,40,45,65,85,94,98,101,102], which are summarized in Appendix B. However,
 350 further study of the sustainable concrete application is needed by comparing the different
 351 chemical composition and particle characteristics. De Brito et al. [46] presented a ternary
 352 phase diagram to provide the chemical composition of various binder types from 81
 353 publications. As shown in Fig. 11, the chemical composition of industrial wastes are
 354 diversities and significantly determined on the source of the raw materials, and it cannot
 355 directly be replaced with the equivalent mass of cement because of the amorphous particles is
 356 different from the cement. Furthermore, certain experimental studies of sustainable
 357 optimization were focused on cost and environmental impact [53,76,84,88,91].



358
 359 **Fig. 11** $\text{CaO-SiO}_2\text{-Al}_2\text{O}_3$ ternary phase diagram for the cement blends of sustainable concrete.
 360 Adapted from [46]

361 4. Summary and discussion

362 Based on the 80 applications of RSMs in the existing literature and its analysis, some
363 critical information of statistical models to optimize the mixture proportioning of
364 cement-based materials, including RSM method, test specimen, factors (independent variables)
365 and its responses (dependent variables), were collected. The summary is listed in Appendix B.

366 4.1 Selection of design strategy

367 As it is shown in Appendix B, CCD is the most popular method for mixture
368 proportioning optimization in cement-based materials. CCD comprises a two-level factorial
369 design, centre point and a star design in which test points with a distance α from the centre
370 point. CCD provides a considerable high efficiency with up to six factors if all optimizations
371 are carried in parallel instead of sequentially experiments. It is often used to be regarded as a
372 better alternative of the full factorial design because it can offer similar results with a smaller
373 number of experiments [17]. In addition, both linear and quadratic regression models are
374 permitted to be determined by these design strategies, and the interactive effects of various
375 independent factors and critical points (minimum, maximum and saddle points) can be
376 evaluated.

377 Another popular method is simplex design, including the simplex-lattice design and
378 simplex-centroid design. The factors of these strategies are the component of a mixture, and
379 the factor levels are not independent. If there are three ingredients of the mixture, the
380 constrained experimental region is constructed to a trilinear coordinate system as shown in
381 [16,38]. Each of the three sides of the triangle represents a mixture that has only two
382 components, and the missing component labelled on the opposite corner.

383 However, BBD has not been employed as extensive as the above-mentioned strategies in
384 cement-based materials. While in BBD strategy, all points located at a spherical region of

385 radius $\sqrt{2}$. And also, BBD does not contain any corner points of the cubic region to avoid the
386 upper and lower limits of the given constraints. This would be available for BBD when the
387 extreme vertices are prohibitively expensive or impossible to complete owing to the constraints
388 of the experimental conditions.

389 Anyway, the prevalence of CCD usage in cement-based materials is partly attributed to
390 that it is easy to follow the other researcher's steps. As for geopolymer/alkali-activated
391 materials and UHPC with various ingredients and several performance requirements,
392 D-optimal design or Doehlert design [47] or BBD might be a better beneficial strategy.

393 **4.2 Selection of factors and responses**

394 The W/B ratio and mixture components are the prevalent factors in experimental design
395 optimization, then fluidity and strength as the most popularly used response. Each response of
396 mixture optimization is often expressed with a polynomial function of factors such as W/B
397 ratio, cement content, admixture dosage and SCM replacement. Changing of W/B ratio leads
398 to a remarkable variation of concrete properties. In general, selection of the factors and its
399 level should be according to the preliminary tests or practical experience and not depending
400 on the researcher's convenience. Furthermore, performing heavy single-variable studies with
401 the purpose to optimize with three or more factors should be avoided [14].

402 Recently, the multiple response problem of cement-based materials has become a
403 concern. Jiao et al. [38] overlapped several critical contour lines of each response to acquire
404 the multiple performance requirements. Ferdosian and Camoes [31] employed D-optimal
405 design to develop a combined desirability with different important weights for their
406 corresponding solutions. These multi-objective optimization approaches need a further
407 systematic study.

408 Obviously, the choice of the variable levels in the optimization process is more important
409 than the design itself. Every level of RSM must be appropriate and provide valuable
410 information. When the design points are too close together, it will not result in the obvious
411 influence of the corresponding response. On the contrary, if design points are at the extreme
412 point of a reasonable region, the responses are often hard to adopt.

413 **4.3 Selection of experimental domain**

414 Although RSM has many outstanding characteristics and has been widely used for
415 mixture design and process optimization of various experiments, the fitting models can be
416 only suitable for the experimental domain and are not accurate for extrapolation. In addition,
417 discrete variables cannot be selected for experimental optimization. For example, a specific
418 type of SCM or any other mixture components cannot be considered in the mixture
419 optimization problems.

420 In order to overcome the defects of RSM strategy, some researchers attempt to integrate
421 of RSM with other machine learning algorithms, such as artificial neural networks [48-50],
422 fuzzy classification [51]. These combined approaches have been demonstrated experimentally
423 by providing well precision in data learning and prediction. Although these solutions have
424 been used in several other fields, little research has been reported of these applications in
425 mixture proportion optimization.

426 **4.4 Current challenges for the applications of sustainable concrete**

427 In general, reducing the environmental impact and resources consumption of sustainable
428 concrete is related to replace cement clinker with solid wastes, which contains many
429 ingredients and are always subject to multi-performance requirements. Statistical
430 experimental design has been developed to optimize the mixture proportion of sustainable
431 concrete. However, target performance during the optimization process may be mutually

432 exclusive, which leads to numerous redundant works. The combined desirability of various
433 weighted values and their corresponding solutions has been developed a multi-objective
434 optimization [5,31,40,84]. The simultaneous nonlinear optimization with desirability function
435 should be further studied in the future.

436 So far, many multi-variable problems for sustainable concrete optimization have become
437 increasingly common. It is difficult to coordinate the raw materials properties and their
438 dosage are often lacks a theoretical basis. Furthermore, little attention has been focused on the
439 independent factors and their interactions of sustainable concrete applications.

440 **5. Conclusions and Prospective**

441 Based on the review and discussions in this paper, the conclusions can be drawn as
442 below:

443 (1) The RSM is a sequential procedure to provide a suitable approximation for the fitting
444 functional models between various independent factors and their responses. Then,
445 linear, quadratic and interactive relationships of these models can be evaluated. And
446 also, the minimum, the maximum and the saddle points of optimization region can be
447 evaluated available. So, many applications in modelling a variety of cement-based
448 materials field have been attempted, as shown in Appendix B.

449 (2) CCD is the most commonly used method in cement and concrete mixture design.
450 Most studies considered four or less independent variables. The W/B ratio and
451 mixture components are the prevalent factors in experimental design optimization,
452 and then the fluidity and strength as the most popularly used response. However,
453 D-optimal design or BBD or Doehlert design might be better for
454 geopolymer/alkali-activated materials and UHPC with various ingredients and
455 several performance requirements.

- 456 (3) The choice of factors and their levels is very important for experimental optimization
457 by using RSM. Each level should be appropriate and provide valuable information,
458 and it is necessary to assure the responses within the acceptable region of the
459 optimum value.
- 460 (4) The multiple or competing performance requirement of mixture design has become a
461 concern. The in-depth investigations are needed to combine and compare with other
462 modelling techniques. Previous studies investigated the combination of D-optimal
463 method and particle packing models. However, artificial neural network and fuzzy
464 logic for modelling mixture optimization issues may be a promising research
465 direction.
- 466 (5) Further study of sustainable concrete optimization is needed by comparing the
467 different chemical composition and particle characteristics. However, target
468 performance during the optimization process may be mutually exclusive, which leads
469 to numerous redundant works. So, the simultaneous nonlinear optimization with
470 desirability function should be further studied in the future.
- 471 (6) Although plenty of studies have been reported in the previous literature with the
472 laboratory experiment in the cement-based materials field, little attention has focused
473 on the applications in engineering practice. Thus, more attempts relating to the
474 practical project by using RSM are needed.

475 **Acknowledgements**

476 The authors would like to thank for the financial support from the National Science
477 Foundation of China (Grant Nos. 51678209, 41861134010).

478 **Appendix A. List of symbols.**

Symbol	Description
RSM	response surface method
CCD	central composite design
BBD	Box- Behnken design
CCF	face-centred central composite design
ANOVA	analysis of variance
UHPC	ultra-high performance concrete
HPC	high performance concrete
SCC	self-compacting concrete
ASR	alkali-silica reaction
W/B	Water-binder ratio
SCM	supplementary cementitious material
SF	silica fume
FA	fly ash
QP	quartz powder
GBFS	Granulated blast furnace slag
Vca	volume of coarse aggregate
Vfa	volume of fine aggregate
SP	superplasticizer
Fc	28-day compressive strength
Ft	flexure strength

479

480 **Appendix B.** Applications of RSM for mixture optimization of cement-based materials.

RSM method	Specimen	Factors	Response(s)	R ²	Number of experiments	Year	Ref.
CCD	SCC	W/B ratio, Binder, SP, Vca	fluidity, rheology, Fc	slump=0.95, Fc=0.83	15	2000	[52]
Factorial design	mortar	SF, FA, GBFS	SP, setting time, drying shrinkage,fc,cost		13/26*	2002	[53]
CCD	SCC	cement, limestone filler, SP, W/B ratio	fluidity, Fc	slump=0.98, Fc=0.97	21	2002	[54]
BBD	mineral aggregate	six types of silica sand	void content	0.96	54	2003	[55]
Full factorial design	steel fibre reinforced concrete	aspect ratio, volume of steel fibre	fracture energy, characteristic length		10	2004	[56]
CCD	SCC	pulverised fuel ash, SP, cement, W/B ratio	fluidity, rheology, segregation ratio, Fc	slump=0.99, rheology=0.98, segregation ratio=0.99, Fc=0.99	21	2004	[57]
CCD	foam concrete	filler-cement ratio, FA, foam volume	Fc, dry density	Fc=0.958, dry density=0.987	20	2006	[58]
BBD	bridge deck overlay concrete	SF, FA, slag	Fc, Ft, chloride permeability, abrasion resistance		15	2006	[59]
Bucher–Bourgund design	frost-resistant concrete	W/B ratio, entrained air pore, number of cycles	residual strain		7	2007	[60]
simplex centroid design	blends of industrial wastes	red clay, granite waste, kaolin waste	water absorption, shrinkage, modulus of rupture		10/40	2008	[61]
simplex centroid design	HPC	cement, FA, GBFS, SP, Vca, Vfa	fluidity, Fc		78	2009	[49]
CCD	SCC	cement, W/B ratio, FA, SP	Fc, modulus of elasticity	Fc=0.823	31	2009	[62]
simplex centroid design	drilling fluid	Bentonite, low molar carboxymethyl cellulose, high molar carboxymethyl cellulose	apparent viscosity, plastic viscosity		10/30	2010	[63]
BBD	high-strength lightweight concrete	temperature, binder content, binder type	specific gravity, water absorption, crushing strength		18	2011	[64]
fractional factorial design	SCC	binder, W/B, binder type, SP, sand-aggregate ratio	fluidity, Fc, shrinkage, creep		19	2012	[37]

(continued on next page)

RSM method	Specimen	Factors	Reponse(s)	R ²	Number of experiments	Year	Ref.
CCD	recycled masonry and concrete	cement, degree of compaction	moisture content, dry density		13	2012	[65]
CCD	High flowing concrete	GBFS, FA, W/B ratio, SP	fluidity, Fc, Durability	slump=0.9841, Fc=0.9315, carbonaion=0.9717	21	2012	[66]
CCD	SCC	cement, W/B ratio, FA, SP	fluidity, Fc, modulus of elasticity	fluidity=0.905, Fc=0.920, modulus of elasticity=0.818	31	2012	[67]
CCD	oil well cement slurry	SP, SCM, temperature	yield stress, plastic viscosity		40	2012	[68]
BBD	alkali-slag concrete	solution-slag ratio, slag, sand	Air bubble spacing coefficient, Air bubble specific surface area, Grades of freeze-thaw resistance		17	2013	[43]
Factorial design	pervious concrete	W/B ratio, cement, Vca	fresh density, hardened density, void ratio, Fc	fresh density=0.79, hardened density=0.97, void ratio=0.98, Fc=0.87	13	2013	[69]
fractional factorial design	concrete	W/B, cement, fineness modulus of aggregate, SP	Fc		46/92	2013	[70]
CCD	warm mix asphalt	binder, resident, compaction temperature	air void, bulk specific gravity, voids filled with asphalt binder, stability, fluidity	air void=0.94, bulk specific gravity=0.96, stability=0.77, fluidity=0.89	20	2013	[71]
CCD	UHPC	cement, SF	fluidity, Fc	slump=0.9949, Fc=0.9913	13	2013	[36]
simplex lattice design	HPC	cement, grinded dune sand, limestone filler	fluidity, Fc	slump=0.78, Fc=0.91	21	2014	[72]
Factorial design	concrete	FA, metakaolin, testing age	Fc, chloride permeability, sorptivity, water absorption		9	2014	[73]
Full factorial design	concrete	binder, W/B, Vfa/Vca	Fc	0.8	27	2014	[74]
BBD	silicate cement	water-soluble polymer, chemical additive, SP	Fc		27	2014	[75]

(continued on next page)

RSM method	Specimen	Factors	Reponse(s)	R ²	Number of experiments	Year	Ref.
BBD	alkali-slag concrete	alkali, W/B ratio, ground clay	expansion, Fc, Ft, modulus of elasticity	expansion=0.886, Fc=0.889, Ft=0.900, modulus of elasticity=0.847	30	2014	[42]
CCD	normal weight concrete	W/B ratio, Vca, SP	fluidity, Fc, splitting tensile strength, cost	slump=0.992, Fc=0.837, splitting tensile strength=0.825, cost=1.000	20	2014	[76]
CCD	self-compacting UHPC	steel fibre, powder-aggregate ratio	Ft, fluidity	Ft=0.91, fluidity=0.92	20	2014	[35]
CCD	modified asphalt mixture	asphalt, polyethene terephthalate modifier	fluidity, void, stability, bulk specific gravity	slump=0.9880, void=0.9980, stability=0.9853, bulk specific gravity=0.9883	13	2015	[77]
CCD	SCC	binder, W/B ratio, SP	fluidity, Fc, filling capacity, sieve segregation	slump=0.96, Fc=0.86, filling capacity=0.95, sieve segregation=0.94	20	2015	[78]
CCD	SCC	binder, W/B ratio, SCM	fluidity, Fc, segregation factor		27	2015	[79]
CCF	cement paste	W/B ratio, FA/B ratio, nano-iron oxide-to-binder	fluidity, Fc	slump=0.855, Fc=0.852	20	2015	[80]
simplex lattice design	UHPC	cement, sand, SF, QP, SP, steel fibre	fluidity, Ft	slump=0.74, Ft=0.90	53	2015	[15]
BBD	pervious concrete	three admixture	paste thickness, slump, film drying time	paste thickness=0.92, slump=0.89, film drying time=0.69	18	2015	[81]
BBD	alkali-slag concrete	sol ratio, slag, age on fracture toughness	initiation fracture toughness, unstable fracture toughness, crack mouth opening displacement, critical effective crack		17	2015	[41]
simplex lattice design	mortar	cement, SF, nano-silica	fluidity, Fc, Ft, splitting strength, density, absorption, capillary water		13	2016	[82]
simplex lattice design	alkali-activated cement	cement, FA, slag	ASR expansion		17	2016	[16]

(continued on next page)

RSM method	Specimen	Factors	Response(s)	R ²	Number of experiments	Year	Ref.
CCD	concrete	crumb rubber, metakaolin	Fc, water absorption, unit weight	Fc=0.9703, water absorption=0.8751, unit weight=0.8321	9	2016	[83]
CCD	SCC	W/B ratio, cement, Vfa, FA, SP	fluidity, Fc, cost	fluidity=0.9604, Fc=0.9547, cost=1	52	2016	[84]
CCD	UHPC	SF, SP, fibre, cement, W/B	flexural toughness	flexural toughness=0.85	45	2016	[34]
simplex lattice design	geopolymer mortar	FA, GBFS	binder, curing time, curing temperature, Fc		7/14	2017	[40]
simplex lattice design	UHPC	cement, SF, QP, quartz sand	fluidity, Fc, air void	slump=0.99, Fc=0.99, air void=0.80	10	2017	[44]
CCF	eco-friendly UHPC	micro-coral sand, coral sand	Fc	0.97	10	2017	[30]
CCD	SCC	W/B, marble powder-cement ratio	fluidity, Fc		33	2017	[85]
CCF	mortar	clinker, FA, debit grinding agent	Fc	0.98	15	2017	[86]
CCD	warm mix asphalt	compaction temperature, test temperature	adhesion failure, direct tensile strength, fracture energy, broken aggregate		11/22	2017	[87]
CCD	high-strength SCC	W/B, cement, FA, SP, Vfa	Fc, fluidity, cost	Fc=0.955, fluidity=0.960, cost=1	52	2017	[88]
CCF	UHPC	QP, quartz sand, water curing	Fc, Ft	Fc=0.984, Ft=0.830	16	2017	[32]
CCD	UHPC	SF, sand, ultra-fine fly ash	fluidity, Fc	slump=0.9596, fc=0.9568	28	2017	[31]
simplex centroid design	low carbon cementitious material	cement, mineral admixture, hydrated lime	fluidity, Fc, hydration heat, porosity, non-evaporable water		7	2018	[89]
simplex centroid design	alkali-activated concrete	gravel, sand	bulk density		7	2018	[39]
simplex centroid design	concrete	Vca, Vfa, paste, cement, FA, slag	rheology, Fc		16	2018	[38]
BBD	grout material	cement, FA, microsilica, metakaolin	fluidity, Fc, Ft, shrinkage	slump=0.9647, Fc=0.9810, Ft=0.7966, shrinkage=0.8053	16	2018	[90]
BBD	foamed concrete	cement, foam	Fc, dry density, cost		15	2018	[91]

(continued on next page)

RSM method	Specimen	Factors	Reponse(s)	R ²	Number of experiments	Year	Ref.
simplex centroid design	SCC	SP, stone powder, gravel, sand, cement	fluidity, Fc		42	2018	[92]
CCD	geopolymeric binder	modulus of sodium silicate, liquid, mineral admixture	Fc	0.9736	15	2018	[27]
CCD	alkali-activated slag mortar	Na ₂ O, glass powder	Fc, Ft	Fc=0.9678, Ft=0.9754	13	2018	[26]
CCD	geopolymer composite	NaOH molarity, Na ₂ SiO ₃ , curing temperature	Fc, elastic modulus, Ft, flexural toughness, ductility index, tensile first crack strength, ultimate tensile strength, tensile strain capacity	Fc=0.9951, elastic modulus=0.9977, Ft=0.9924, flexural toughness=0.9837, ductility index=0.9731, tensile first crack strength=0.9876, ultimate tensile strength=0.9791, tensile strain capacity=0.9850	20	2018	[25]
CCD	rubbercrete mixture	W/B ratio, crumb rubber	fluidity, unit weight, void, Fc		45	2018	[20]
CCD	self-consolidating mortar	SF, slag, SP, W/B ratio	fluidity, Fc, segregation	slump=0.9589, Fc=0.8561, segregation=0.8141	30	2018	[93]
CCD	normal concrete	two types of plastic waste aggregate	fluidity, Fc	slump=0.8198, Fc=0.9750	13	2018	[94]
CCF	polymer nanocomposite-modified asphalt	nanosilica additive, temperature	complex modulus, phase angle, viscosity	complex modulus=0.9995, phase angle=0.9989, viscosity=0.9995	13	2019	[95]
Full factorial design	SCC	cement, FA, W/B, SP	fluidity, Fc	slump=0.9319, Fc=0.9343	18	2019	[51]
CCD	recycled concrete aggregate	cement, slump, recycled coarse aggregate	Fc	0.9881	17	2019	[96]
CCD	geopolymer	sisal fibre, activator, curing time	Fc, toughness, modulus of elasticity		18	2019	[24]

(continued on next page)

RSM method	Specimen	Factors	Reponse(s)	R ²	Number of experiments	Year	Ref.
CCRD	fibre reinforced concrete	aspect ratio, cement, W/B ratio	fluidity, Fc, Ft, split tensile strength, water absorption	slump=0.98, Fc=0.95, Ft=0.98, split tensile strength=0.93, water absorption=0.8640	20	2019	[97]
CCF	alkali-activated paste	slag, anhydrous sodium metasilicate activator	Fc, Ft, water absorption	Fc=0.9856, Ft=0.9913, water absorption=0.8994	15	2019	[23]
CCD	geopolymer concrete	Vfa, FA, waste foundry sand	Fc	0.99	14	2019	[22]
CCD	UHPC	porous aggregate, shrinkage reducing admixture	autogenous shrinkage	0.9296	11	2019	[29]
CCF	UHPC	nano-silica, waste glass powder	fluidity, Fc, drying shrinkage	slump=0.93, Fc=0.98, drying shrinkage=0.96	10	2019	[33]
CCD	eco-efficient SCC	limestone powder, FA, SP	fluidity, Fc	slump=0.9679, Fc=0.9695	20	2019	[98]
BBD	pervious concrete	aggregate size	bulk density, apparent density, void		24	2020	[99]
BBD	blended paste	cement, SF, FA, QP	fluidity, rheology, hydration heat, Fc, drying shrinkage	slump=0.9613, rheology=0.9818, hydration heat=0.9975, Fc=0.9955, drying shrinkage=0.9459	16	2020	[5]
CCF	concrete	manufactured sand, metakaolin, waste paper sludge ash	Fc, permeability coefficient, sorptivity	permeability coefficient=0.9745,	17	2020	[100]
CCD	cementitious composites	cement, curing time	Fc	0.97	14	2020	[101]
CCD	strain-hardening UHPC	W/B ratio, SCM, distribution modulus	fluidity, rheology, Fc, fracture toughness		20/60	2020	[28]
CCD	geopolymer mortar	molarity, binder, sodium silicate to sodium hydroxide ratio	Fc, drying shrinkage	Fc=0.9063, drying shrinkage=0.9296	27	2020	[102]

481 *Note: * two groups, 11 mixtures for each one.*

482
483
484

485
 486
 487
 488
 489
 490
 491
 492
 493
 494
 495
 496
 497
 498
 499
 500
 501
 502
 503
 504
 505
 506
 507
 508
 509
 510
 511
 512
 513
 514
 515
 516
 517
 518

References:

- [1] M.A. DeRousseau, J.R. Kasprzyk, W.V. Srubar: Computational design optimization of concrete mixtures: A review. *Cement and Concrete Research*, 109 (2018) 42-53. <https://doi.org/10.1016/j.cemconres.2018.04.007>
- [2] Chinese National Institute of Standardization, Specification for mix proportion design of ordinary concrete, JGJ 55-2011, Beijing, 2011.
- [3] Chinese National Institute of Standardization, Specification for mix proportion design of masonry mortar, JGJ/T 98-2010, Beijing, 2010.
- [4] Chinese National Institute of Standardization, Specification for mix proportion design of cement soil, JGJ/T 233-2011, Beijing, 2011.
- [5] Z. Li, D. Lu, X. Gao: Multi-objective optimization of gap-graded cement paste blended with supplementary cementitious materials using response surface methodology. *Construction and Building Materials*, 248 (2020) 118552. <https://doi.org/10.1016/j.conbuildmat.2020.118552>
- [6] Q. Chen, H. Wang, H. Li, Z. Jiang, H. Zhu, J.W. Ju, Z. Yan: Multiscale modelling for the ultra-high performance concrete: From hydration kinetics to macroscopic elastic moduli. *Construction and Building Materials*, 247 (2020). <https://doi.org/10.1016/j.conbuildmat.2020.118541>
- [7] C. Shi, Z. Wu, J. Xiao, D. Wang, Z. Huang, Z. Fang: A review on ultra high performance concrete: Part I. Raw materials and mixture design. *Construction and Building Materials*, 101 (2015) 741-751. <https://doi.org/10.1016/j.conbuildmat.2015.10.088>
- [8] H. Wei, A. Zhou, T. Liu, D. Zou, H. Jian: Dynamic and environmental performance of eco-friendly ultra-high performance concrete containing waste cathode ray tube glass as a substitution of river sand. *Resources, Conservation and Recycling*, 162 (2020) 105021. <https://doi.org/10.1016/j.resconrec.2020.105021>
- [9] Z. Mo, X. Gao, A. Su: Mechanical performances and microstructures of metakaolin contained UHPC matrix under steam curing conditions. *Construction and Building Materials*, (2020) 121112. <https://doi.org/10.1016/j.conbuildmat.2020.121112>
- [10] J.H. Son, J.W. Baek, A.E. Sy Choi, H.S. Park: Thiomer solidification of an ASR bottom ash: Optimization based on compressive strength and the characterization of heavy metal leaching. *Journal of Cleaner Production*, 166 (2017) 12-20. <https://doi.org/10.1016/j.jclepro.2017.07.113>
- [11] M. Simon, K. Snyder, F. G, Advances in concrete mixture optimization, Concrete Durability and Repair Technology Conference, Scotland, 1999, pp.21-32.
- [12] D. C. Montgomery. Design and Analysis of Experiments (6nd Ed), Journal of the American Statistical Association, 2000, 16(2).

- 519 [13] S. Karimifard, M.R. Alavi Moghaddam: Application of response surface methodology in
520 physicochemical removal of dyes from wastewater: A critical review. *Science of the Total*
521 *Environment*, 640-641 (2018) 772-797. <https://doi.org/10.1016/j.scitotenv.2018.05.355>
- 522 [14] A. Khuri, S. Mukhopadhyay: Response surface methodology. *Wiley interdisciplinary reviews:*
523 *computational statistics*, 2 (2010) 128-149. <https://doi.org/10.1002/wics.73>
- 524 [15] E. Ghafari, H. Costa, E. Júlio: Statistical mixture design approach for eco-efficient UHPC. *Cement*
525 *and Concrete Composites*, 55 (2015) 17-25. <https://doi.org/10.1016/j.cemconcomp.2014.07.016>
- 526 [16] Z. Shi, C. Shi, R. Zhao, D. Wang, F. He: Factorial design method for designing ternary composite
527 cements to mitigate ASR expansion. *Journal of Materials in Civil Engineering*, 28 (2016) 4016064.
528 [https://doi.org/10.1061/\(ASCE\)MT.1943-5533.0001568](https://doi.org/10.1061/(ASCE)MT.1943-5533.0001568)
- 529 [17] K.M. Sharif, M.M. Rahman, J. Azmir, A. Mohamed, M.H.A. Jahurul, F. Sahena, I.S.M. Zaidul:
530 Experimental design of supercritical fluid extraction - a review. *Journal of Food Engineering*, 124
531 (2014) 105-116. <https://doi.org/10.1016/j.jfoodeng.2013.10.003>
- 532 [18] S. Bouzalakos, A.W.L. Dudeney, B.K.C. Chan: Formulating and optimising the compressive strength
533 of controlled low-strength materials containing mine tailings by mixture design and response surface
534 methods. *Minerals Engineering*, 53 (2013) 48-56. <https://doi.org/10.1016/j.mineng.2013.07.007>
- 535 [19] J.S.J. van Deventer, J.L. Provis, P. Duxson: Technical and commercial progress in the adoption of
536 geopolymer cement. *Minerals Engineering*, 29 (2012) 89-104.
537 <https://doi.org/10.1016/j.mineng.2011.09.009>
- 538 [20] B.S. Mohammed, V.C. Khed, M.F. Nuruddin: Rubbercrete mixture optimization using response
539 surface methodology. *Journal of Cleaner Production*, 171 (2018) 1605-1621.
540 <https://doi.org/10.1016/j.jclepro.2017.10.102>
- 541 [21] P. Zhang, K. Wang, Q. Li, J. Wang, Y. Ling: Fabrication and engineering properties of concretes
542 based on geopolymers/alkali-activated binders - a review. *Journal of Cleaner Production*, 258 (2020)
543 120896. <https://doi.org/10.1016/j.jclepro.2020.120896>
- 544 [22] M. Venkatesan, Q. Zaib, I.H. Shah, H.S. Park: Optimum utilization of waste foundry sand and fly ash
545 for geopolymer concrete synthesis using D-optimal mixture design of experiments. *Resources,*
546 *Conservation and Recycling*, 148 (2019) 114-123. <https://doi.org/10.1016/j.resconrec.2019.05.008>
- 547 [23] B.S. Mohammed, S. Haruna, M. Mubarak Bn Abdul Wahab, M.S. Liew: Optimization and
548 characterization of cast in-situ alkali-activated pastes by response surface methodology. *Construction*
549 *and Building Materials*, 225 (2019) 776-787. <https://doi.org/10.1016/j.conbuildmat.2019.07.267>
- 550 [24] L.C. Da Silva Alves, R.A. Dos Reis Ferreira, L. Bellini Machado, L.A. de Castro Motta:
551 Optimization of metakaolin-based geopolymer reinforced with sisal fibers using response surface
552 methodology. *Industrial Crops and Products*, 139 (2019) 111551.

- 553 <https://doi.org/10.1016/j.indcrop.2019.111551>
- 554 [25] M. Zahid, N. Shafiq, M.H. Isa, L. Gil: Statistical modeling and mix design optimization of fly ash
555 based engineered geopolymer composite using response surface methodology. *Journal of Cleaner*
556 *Production*, 194 (2018) 483-498. <https://doi.org/10.1016/j.jclepro.2018.05.158>
- 557 [26] L. Zhang, Y. Yue: Influence of waste glass powder usage on the properties of alkali-activated slag
558 mortars based on response surface methodology. *Construction and Building Materials*, 181 (2018)
559 527-534. <https://doi.org/10.1016/j.conbuildmat.2018.06.040>
- 560 [27] T. Revathi, R. Jeyalakshmi, N.P. Rajamane: Geopolymeric binder: The effect of silica fume addition
561 on Fly activation by using response surface methodology. *Materials Today: Proceedings*, 5 (2018)
562 8727-8734. <https://doi.org/10.1016/j.matpr.2017.12.299>
- 563 [28] K. Ragalwar, W.F. Heard, B.A. Williams, R. Ranade: Significance of the particle size distribution
564 modulus for strain-hardening-ultra-high performance concrete (SH-UHPC) matrix design.
565 *Construction and Building Materials*, 234 (2020) 117423.
566 <https://doi.org/10.1016/j.conbuildmat.2019.117423>
- 567 [29] Y. Sun, R. Yu, Z. Shui, X. Wang, D. Qian, B. Rao, J. Huang, Y. He: Understanding the porous
568 aggregates carrier effect on reducing autogenous shrinkage of Ultra-High Performance Concrete
569 (UHPC) based on response surface method. *Construction and Building Materials*, 222 (2019)
570 130-141. <https://doi.org/10.1016/j.conbuildmat.2019.06.151>
- 571 [30] X. Wang, R. Yu, Z. Shui, Q. Song, Z. Zhang: Mix design and characteristics evaluation of an
572 eco-friendly Ultra-High Performance Concrete incorporating recycled coral based materials. *Journal*
573 *of Cleaner Production*, 165 (2017) 70-80. <https://doi.org/10.1016/j.jclepro.2017.07.096>
- 574 [31] I. Ferdosian, A. Camoes: Eco-efficient ultra-high performance concrete development by means of
575 response surface methodology. *Cement & Concrete Composites*, 84 (2017) 146-156.
576 <https://doi.org/10.1016/j.cemconcomp.2017.08.019>
- 577 [32] M.A. Mosaberpanah, O. Eren: Effect of quartz powder, quartz sand and water curing regimes on
578 mechanical properties of UHPC using response surface modelling. *Advances in Concrete*
579 *Construction*, 5 (2017) 481-492. <https://doi.org/10.12989/acc.2017.5.5.481>
- 580 [33] M.A. Mosaberpanah, O. Eren, A.R. Tarassoly: The effect of nano-silica and waste glass powder on
581 mechanical, rheological, and shrinkage properties of UHPC using response surface methodology.
582 *Journal of Materials Research and Technology*, 8 (2019) 804-811.
583 <https://doi.org/10.1016/j.jmrt.2018.06.011>
- 584 [34] M.A. Mosaberpanah, O. Eren: Statistical flexural toughness modeling of ultra high performance
585 concrete using response surface method. *Computers and Concrete*, 17 (2016) 477-488.
586 <https://doi.org/10.12989/cac.2016.17.4.477>

- 587 [35] E. Ghafari, H. Costa, E. Júlio: RSM-based model to predict the performance of self-compacting
588 UHPC reinforced with hybrid steel micro-fibers. *Construction and Building Materials*, 66 (2014)
589 375-383. <https://doi.org/10.1016/j.conbuildmat.2014.05.064>
- 590 [36] M.A.A. Aldahdooh, N.M. Bunnori, M.A.M. Johari: Evaluation of ultra-high-performance-fiber
591 reinforced concrete binder content using the response surface method. *Materials & Design*, 52 (2013)
592 957-965. <https://doi.org/10.1016/j.matdes.2013.06.034>
- 593 [37] W. Long, G. Lemieux, S. Hwang, K.H. Khayat: Statistical models to predict fresh and hardened
594 properties of self-consolidating concrete. *Materials and Structures*, 45 (2012) 1035-1052.
595 <https://doi.org/10.1617/s11527-011-9815-9>
- 596 [38] D. Jiao, C. Shi, Q. Yuan, X. An, Y. Liu: Mixture design of concrete using simplex centroid design
597 method. *Cement and Concrete Composites*, 89 (2018) 76-88.
598 <https://doi.org/10.1016/j.cemconcomp.2018.03.001>
- 599 [39] N. Li, C. Shi, Z. Zhang, D. Zhu, H. Hwang, Y. Zhu, T. Sun: A mixture proportioning method for the
600 development of performance-based alkali-activated slag-based concrete. *Cement & Concrete*
601 *Composites*, 93 (2018) 163-174. <https://doi.org/10.1016/j.cemconcomp.2018.07.009>
- 602 [40] K. Mermerdas, Z. Algin, S.M. Oleiwi, D.E. Nassani: Optimization of lightweight GGBFS and FA
603 geopolymer mortars by response surface method. *Construction and Building Materials*, 139 (2017)
604 159-171. <https://doi.org/10.1016/j.conbuildmat.2017.02.050>
- 605 [41] Q. Li, L. Cai, Y. Fu, H. Wang, Y. Zou: Fracture properties and response surface methodology model
606 of alkali-slag concrete under freeze - thaw cycles. *Construction and Building Materials*, 93 (2015)
607 620-626. <https://doi.org/10.1016/j.conbuildmat.2015.06.037>
- 608 [42] F. Bektas, B.A. Bektas: Analyzing mix parameters in ASR concrete using response surface
609 methodology. *Construction and Building Materials*, 66 (2014) 299-305.
610 <https://doi.org/10.1016/j.conbuildmat.2014.05.055>
- 611 [43] L. Cai, H. Wang, Y. Fu: Freeze - thaw resistance of alkali - slag concrete based on response surface
612 methodology. *Construction and Building Materials*, 49 (2013) 70-76.
613 <https://doi.org/10.1016/j.conbuildmat.2013.07.045>
- 614 [44] N.A. Soliman, A. Tagnit-Hamou: Using particle packing and statistical approach to optimize
615 Eco-Efficient Ultra-High-Performance concrete. *Aci Materials Journal*, 114 (2017) 847-858.
616 <https://doi.org/10.14359/51701001>
- 617 [45] L. Qin, X. Gao, A. Su, Q. Li: Effect of carbonation curing on sulfate resistance of cement-coal
618 gangue paste. *Journal of Cleaner Production*, 278 (2021) 123897.
619 <https://doi.org/10.1016/j.jclepro.2020.123897>
- 620 [46] J. de Brito, R. Kurda: The past and future of sustainable concrete: A critical review and new

- 621 strategies on cement-based materials. *Journal of Cleaner Production*, (2020) 123558.
622 <https://doi.org/10.1016/j.jclepro.2020.123558>
- 623 [47] D.B. Hibbert: Experimental design in chromatography: A tutorial review. *Journal of Chromatography*
624 *B-Analytical Technologies in the Biomedical and Life Sciences*, 910 (2012) 2-13.
625 <https://doi.org/10.1016/j.jchromb.2012.01.020>
- 626 [48] W.E. Elemam, A.H. Abdelraheem, M.G. Mahdy, A.M. Tahwia: Optimizing fresh properties and
627 compressive strength of self-consolidating concrete. *Construction and Building Materials*, 249
628 (2020). <https://doi.org/10.1016/j.conbuildmat.2020.118781>
- 629 [49] I. Yeh: Optimization of concrete mix proportioning using a flattened simplex – centroid mixture
630 design and neural networks. *Engineering with Computers*, 25 (2009) 179-190.
631 <https://doi.org/10.1007/s00366-008-0113-2>
- 632 [50] Z.M. Sbartai, S. Laurens, S.M. Elachachi, C. Payan: Concrete properties evaluation by statistical
633 fusion of NDT techniques. *Construction and Building Materials*, 37 (2012) 943-950.
634 <https://doi.org/10.1016/j.conbuildmat.2012.09.064>
- 635 [51] S. Selvaraj, S. Selvaraj, S. Sivaraman, S. Sivaraman: Prediction model for optimized self-compacting
636 concrete with fly ash using response surface method based on fuzzy classification. *Neural*
637 *Computing and Applications*, 31 (2019) 1365-1373. <https://doi.org/10.1007/s00521-018-3575-1>
- 638 [52] K.H. Khayat, A. Ghezal, M.S. Hadriche: Utility of statistical models in proportioning
639 self-consolidating concrete. *Materials and Structures*, 33 (2000) 338-344.
640 <https://doi.org/10.1007/BF02479705>
- 641 [53] M.L. Nehdi, J. Summer: Optimization of ternary cementitious mortar blends using factorial
642 experimental plans. *Materials and Structures*, 35 (2002) 495-503.
643 <https://doi.org/10.1007/BF02483137>
- 644 [54] A. Ghezal, K.H. Khayat: Optimizing self-consolidating concrete with limestone filler by using
645 statistical factorial design methods. *Aci Materials Journal*, 99 (2002) 264-272.
- 646 [55] M. Muthukumar, D. Mohan, M. Rajendran: Optimization of mix proportions of mineral aggregates
647 using Box Behnken design of experiments. *Cement & Concrete Composites*, 25 (2003) 751-758.
648 [https://doi.org/10.1016/S0958-9465\(02\)00116-6](https://doi.org/10.1016/S0958-9465(02)00116-6)
- 649 [56] F. Bayramov, C. Taşdemir, M.A. Taşdemir: Optimisation of steel fibre reinforced concretes by
650 means of statistical response surface method. *Cement and Concrete Composites*, 26 (2004) 665-675.
651 [https://doi.org/10.1016/S0958-9465\(03\)00161-6](https://doi.org/10.1016/S0958-9465(03)00161-6)
- 652 [57] M. Sonebi: Medium strength self-compacting concrete containing fly ash: Modelling using factorial
653 experimental plans. *Cement and Concrete Research*, 34 (2004) 1199-1208.
654 <https://doi.org/10.1016/j.cemconres.2003.12.022>

- 655 [58] E.K.K. Nambiar, K. Ramamurthy: Models relating mixture composition to the density and strength of
656 foam concrete using response surface methodology. *Cement and Concrete Composites*, 28 (2006)
657 752-760. <https://doi.org/10.1016/j.cemconcomp.2006.06.001>
- 658 [59] J.P. Won, J.M. Seo, C.G. Park, J.H. Kim: Statistical optimisation and durability characteristics of
659 bridge deck overlay concrete. *Magazine of Concrete Research*, 58 (2006) 601-608.
660 <https://doi.org/10.1680/mac.2006.58.9.601>
- 661 [60] T. Cho: Prediction of cyclic freeze - thaw damage in concrete structures based on response surface
662 method. *Construction and Building Materials*, 21 (2007) 2031-2040.
663 <https://doi.org/10.1016/j.conbuildmat.2007.04.018>
- 664 [61] R.R. Menezes, H.G.M. Neto, L.N.L. Santana, H.L. Lira, H.S. Ferreira, G.A. Neves: Optimization of
665 wastes content in ceramic tiles using statistical design of mixture experiments. *Journal of the*
666 *European Ceramic Society*, 28 (2008) 3027-3039.
667 <https://doi.org/10.1016/j.jeurceramsoc.2008.05.007>
- 668 [62] A.N.S. Al Qadi, K. Nasharuddi, H. Al-Mattarn, Q.N.S. AL-Kadi: Statistical models for hardened
669 properties of Self-Compacting concrete. *American Journal of Engineering and Applied Sciences*, 2
670 (2009) 764-770. <https://doi.org/10.3844/ajeassp.2009.764.770>
- 671 [63] R.R. Menezes, L.N. Marques, L.A. Campos, H.S. Ferreira, L.N.L. Santana, G.A. Neves: Use of
672 statistical design to study the influence of CMC on the rheological properties of bentonite
673 dispersions for water-based drilling fluids. *Applied Clay Science*, 49 (2010) 13-20.
674 <https://doi.org/10.1016/j.clay.2010.03.013>
- 675 [64] N.U. Kockal, T. Ozturan: Optimization of properties of fly ash aggregates for high-strength
676 lightweight concrete production. *Materials & Design*, 32 (2011) 3586-3593.
677 <https://doi.org/10.1016/j.matdes.2011.02.028>
- 678 [65] D.X. Xuan, L.J.M. Houben, A.A.A. Molenaar, Z.H. Shui: Mixture optimization of cement treated
679 demolition waste with recycled masonry and concrete. *Materials and Structures*, 45 (2012) 143-151.
680 <https://doi.org/10.1617/s11527-011-9756-3>
- 681 [66] M. Li, Y. Chen, Y. Chan, L.H. Vihn: A study of statistical models application for mixture of
682 high-flowing concrete. *Journal of Marine Science and Technology-Taiwan*, 20 (2012) 325-335.
- 683 [67] A.N.S. Alqadi, K.N.B. Mustapha, S. Naganathan, Q.N.S. Al-Kadi: Uses of central composite design
684 and surface response to evaluate the influence of constituent materials on fresh and hardened
685 properties of self-compacting concrete. *KSCE Journal of Civil Engineering*, 16 (2012) 407-416.
686 <https://doi.org/10.1007/s12205-012-1308-z>
- 687 [68] A. Shahriar, M.L. Nehdi: Optimization of rheological properties of oil well cement slurries using
688 experimental design. *Materials and Structures*, 45 (2012) 1403-1423.

- 689 <https://doi.org/10.1617/s11527-012-9841-2>
- 690 [69] M. Sonebi, M.T. Bassuoni: Investigating the effect of mixture design parameters on pervious
 691 concrete by statistical modelling. *Construction and Building Materials*, 38 (2013) 147-154.
 692 <https://doi.org/10.1016/j.conbuildmat.2012.07.044>
- 693 [70] M.T. Cihan, A. Güner, N. Yüzer: Response surfaces for compressive strength of concrete.
 694 *Construction and Building Materials*, 40 (2013) 763-774.
 695 <https://doi.org/10.1016/j.conbuildmat.2012.11.048>
- 696 [71] M.O. Hamzah, B. Golchin, C.T. Tye: Determination of the optimum binder content of warm mix
 697 asphalt incorporating Rediset using response surface method. *Construction and Building Materials*,
 698 47 (2013) 1328-1336. <https://doi.org/10.1016/j.conbuildmat.2013.06.023>
- 699 [72] R. Zaitri, M. Bederina, T. Bouziani, Z. Makhoulfi, M. Hadjoudja: Development of high performances
 700 concrete based on the addition of grinded dune sand and limestone rock using the mixture design
 701 modelling approach. *Construction and Building Materials*, 60 (2014) 8-16.
 702 <https://doi.org/10.1016/j.conbuildmat.2014.02.062>
- 703 [73] E. Güneyisi, M. Gesoğlu, Z. Algin, K. Mermerdaş: Optimization of concrete mixture with hybrid
 704 blends of metakaolin and fly ash using response surface method. *Composites Part B*, 60 (2014)
 705 707-715. <https://doi.org/10.1016/j.compositesb.2014.01.017>
- 706 [74] S. Ahmad, S.A. Alghamdi: A statistical approach to optimizing concrete mixture design.
 707 *TheScientificWorld*, 2014 (2014) 561537-561539. <https://doi.org/10.1155/2014/561539>
- 708 [75] J. Zheng, G. Shao, X. Shen: Synergistic interactions of chemical additives on the strength
 709 development of silicate cement by a box - behnken model optimization. *Journal of Applied Polymer
 710 Science*, 131 (2014) n/a-n/a. <https://doi.org/10.1002/app.41071>
- 711 [76] B. Simsek, Y.T. Ic, E.H. Simsek, A.B. Guvenc: Development of a graphical user interface for
 712 determining the optimal mixture parameters of normal weight concretes: A response surface
 713 methodology based quadratic programming approach. *Chemometrics and Intelligent Laboratory
 714 Systems*, 136 (2014) 1-9. <https://doi.org/10.1016/j.chemolab.2014.05.001>
- 715 [77] T. Baghaee Moghaddam, M. Soltani, M.R. Karim, H. Baaj: Optimization of asphalt and modifier
 716 contents for polyethylene terephthalate modified asphalt mixtures using response surface
 717 methodology. *Measurement*, 74 (2015) 159-169. <https://doi.org/10.1016/j.measurement.2015.07.012>
- 718 [78] A. Lotfy, K.M.A. Hossain, M. Lachemi: Statistical models for the development of optimized furnace
 719 slag lightweight aggregate self-consolidating concrete. *Cement and Concrete Composites*, 55 (2015)
 720 169-185. <https://doi.org/10.1016/j.cemconcomp.2014.09.009>
- 721 [79] A.A. Abouhussien, A.A.A. Hassan: Optimizing the durability and service life of self-consolidating
 722 concrete containing metakaolin using statistical analysis. *Construction and Building Materials*, 76

- 723 (2015) 297-306. <https://doi.org/10.1016/j.conbuildmat.2014.12.010>
- 724 [80] L. Soto-Perez, V. Lopez, S.S. Hwang: Response Surface Methodology to optimize the cement paste
725 mix design: Time-dependent contribution of fly ash and nano-iron oxide as admixtures. *Materials &*
726 *Design*, 86 (2015) 22-29. <https://doi.org/10.1016/j.matdes.2015.07.049>
- 727 [81] B.E. Jimma, P.R. Rangaraju: Chemical admixtures dose optimization in pervious concrete paste
728 selection - a statistical approach. *Construction and Building Materials*, 101 (2015) 1047-1058.
729 <https://doi.org/10.1016/j.conbuildmat.2015.10.003>
- 730 [82] M.F.A. El Hameed, M.F. Ghazy, M.A.A.A. Elaty: Cement mortar with nanosilica: Experiments with
731 mixture design method. *Aci Materials Journal*, 113 (2016) 43-53. <https://doi.org/10.14359/51688632>
- 732 [83] O. Rezaifar, M. Hasanzadeh, M. Gholhaki: Concrete made with hybrid blends of crumb rubber and
733 metakaolin: Optimization using Response Surface Method. *Construction and Building Materials*,
734 123 (2016) 59-68. <https://doi.org/10.1016/j.conbuildmat.2016.06.047>
- 735 [84] A. Khan, J. Do, D. Kim: Cost effective optimal mix proportioning of high strength self compacting
736 concrete using response surface methodology. *Computers and Concrete*, 17 (2016) 629-648.
737 <https://doi.org/10.12989/cac.2016.17.5.629>
- 738 [85] K.E. Alyamac, E. Ghafari, R. Ince: Development of eco-efficient self-compacting concrete with
739 waste marble powder using the response surface method. *Journal of Cleaner Production*, 144 (2017)
740 192-202. <https://doi.org/10.1016/j.jclepro.2016.12.156>
- 741 [86] N.H. Mtarfi, Z. Rais, M. Taleb, K.M. Kada: Effect of fly ash and grading agent on the properties of
742 mortar using response surface methodology. *Journal of Building Engineering*, 9 (2017) 109-116.
743 <https://doi.org/10.1016/j.jobe.2016.12.004>
- 744 [87] M.O. Hamzah, S.Y. Teh, B. Golchin, J. Voskuilen: Use of imaging technique and direct tensile test to
745 evaluate moisture damage properties of warm mix asphalt using response surface method.
746 *Construction and Building Materials*, 132 (2017) 323-334.
747 <https://doi.org/10.1016/j.conbuildmat.2016.11.092>
- 748 [88] A. Khan, J. Do, D. Kim: Experimental optimization of High-Strength Self-Compacting concrete
749 based on D-Optimal design. *Journal of Construction Engineering and Management*, 143 (2017).
750 [https://doi.org/10.1061/\(ASCE\)CO.1943-7862.0001230](https://doi.org/10.1061/(ASCE)CO.1943-7862.0001230)
- 751 [89] M. Wu, Y. Zhang, G. Liu, Z. Wu, Y. Yang, W. Sun: Experimental study on the performance of
752 lime-based low carbon cementitious materials. *Construction & building materials*, 168 (2018)
753 780-793. <https://doi.org/10.1016/j.conbuildmat.2018.02.156>
- 754 [90] M. Shamsuddoha, G. Hüsken, W. Schmidt, H. Kühne, M. Baeßler: Ternary mix design of grout
755 material for structural repair using statistical tools. *Construction and Building Materials*, 189 (2018)
756 170-180. <https://doi.org/10.1016/j.conbuildmat.2018.08.156>

- 757 [91] S. Asadzadeh, S. Khoshbayan: Multi-objective optimization of influential factors on production
758 process of foamed concrete using Box-Behnken approach. *Construction and Building Materials*, 170
759 (2018) 101-110. <https://doi.org/10.1016/j.conbuildmat.2018.02.189>
- 760 [92] A. Habibi, J. Ghomashi: Development of an optimum mix design method for self-compacting
761 concrete based on experimental results. *Construction and Building Materials*, 168 (2018) 113-123.
762 <https://doi.org/10.1016/j.conbuildmat.2018.02.113>
- 763 [93] M. Aziminezhad, M. Mandikhani, M.M. Memarpour: RSM-based modeling and optimization of
764 self-consolidating mortar to predict acceptable ranges of rheological properties. *Construction and*
765 *Building Materials*, 189 (2018) 1200-1213. <https://doi.org/10.1016/j.conbuildmat.2018.09.019>
- 766 [94] M.A.A. Aldahdooh, A. Jamrah, A. Alnuaimi, M.I. Martini, M.S.R. Ahmed, A.S.R. Ahmed: Influence
767 of various plastics-waste aggregates on properties of normal concrete. *Journal of Building*
768 *Engineering*, 17 (2018) 13-22. <https://doi.org/10.1016/j.jobbe.2018.01.014>
- 769 [95] N. Bala, I. Kamaruddin, M. Napiah, M.H. Sutanto: Polymer Nanocomposite-Modified asphalt:
770 Characterisation and optimisation using response surface methodology. *Arabian Journal for Science*
771 *and Engineering*, 44 (2019) 4233-4243. <https://doi.org/10.1007/s13369-018-3377-x>
- 772 [96] A. Hammoudi, K. Moussaceb, C. Belebhouche, F. Dahmoune: Comparison of artificial neural
773 network (ANN) and response surface methodology (RSM) prediction in compressive strength of
774 recycled concrete aggregates. *Construction and Building Materials*, 209 (2019) 425-436.
775 <https://doi.org/10.1016/j.conbuildmat.2019.03.119>
- 776 [97] T.F. Awolusi, O.L. Oke, O.O. Akinkurolere, A.O. Sojobi: Application of response surface
777 methodology: Predicting and optimizing the properties of concrete containing steel fibre extracted
778 from waste tires with limestone powder as filler. *Case Studies in Construction Materials*, 10 (2019)
779 e212. <https://doi.org/10.1016/j.cscm.2018.e00212>
- 780 [98] M.K. Mohammed, A.I. Al-Hadithi, M.H. Mohammed: Production and optimization of eco-efficient
781 self compacting concrete SCC with limestone and PET. *Construction and Building Materials*, 197
782 (2019) 734-746. <https://doi.org/10.1016/j.conbuildmat.2018.11.189>
- 783 [99] Q. Zhang, X. Feng, X. Chen, K. Lu: Mix design for recycled aggregate pervious concrete based on
784 response surface methodology. *Construction and Building Materials*, 259 (2020) 119776.
785 <https://doi.org/10.1016/j.conbuildmat.2020.119776>
- 786 [100] S. Vasudevan, V. Poornima, M. Balachandran: Influence of admixtures on properties of concrete and
787 optimization using response surface methodology. *Materials Today: Proceedings*, 24 (2020) 650-661.
788 <https://doi.org/10.1016/j.matpr.2020.04.319>
- 789 [101] C. Yan, H. Zhao, J. Zhang, S. Liu, Z. Yang: The cementitious composites using calcium silicate slag
790 as partial cement. *Journal of Cleaner Production*, 256 (2020).
791 <https://doi.org/10.1016/j.jclepro.2020.120514>

- 792 [102] K. Mermerdaş, Z. Algın, Ş. Ekmen: Experimental assessment and optimization of mix parameters of
793 fly ash-based lightweight geopolymer mortar with respect to shrinkage and strength. Journal of
794 Building Engineering, 31 (2020) 101351. <https://doi.org/10.1016/j.jobbe.2020.101351>
795

Journal Pre-proof

Highlights

- Applications of statistical experimental optimization of cement-based materials are reviewed
- The characteristics of the applications of mixture optimization are summarized in table
- A critical discussion of mixture optimization and sustainable concrete application is presented

Declaration of Competing Interest

The authors declare that they have no known competing financial interests or personal relationships that could have appeared to influence the work reported in this paper.

Journal Pre-proof